



PERGAMON

International Journal of Solids and Structures 39 (2002) 4311–4326

INTERNATIONAL JOURNAL OF
SOLIDS and
STRUCTURES

www.elsevier.com/locate/ijsolstr

Three-dimensional stress constraint in an elastic plate with a notch

A. Kotousov ^a, C.H. Wang ^{b,*}

^a Department of Mechanical Engineering, Monash University, P.O. Box 31, Vic. 3800, Australia

^b Aeronautical and Maritime Research Laboratory, Defence Science, and Technology Organisation,
506 Lorimer Street, Fishermans Bend, Vic. 3207, Australia

Received 28 February 2001; received in revised form 4 May 2002

Abstract

This paper presents analytical solutions for the three-dimensional stress distribution around typical stress concentrators in an isotropic plate of arbitrary thickness. Based on the assumption of a generalised plane-strain theory, which assumes that the through-the-thickness extensional strain is uniform in the thickness direction, an exact three-dimensional solution has been obtained for an annulus subjected to arbitrary loading along its edges. Emphasis has been placed on the through-the-thickness stress constraint, which is a pre-requisite to analysing the effect of plate thickness on the elastic-plastic deformation at a notch root. Important results are presented on the effects of the plate thickness and Poisson's ratio on the in-plane stress concentration factor and the out-of-plane stress constraint factor. By extending the theoretical method to a plate with a non-circular notch, an approximate solution has been obtained for the through-the-thickness constraint factor in a plate with a V-shaped notch having a circular tip. The present solutions have been shown to correlate well with numerical results obtained using the finite element method.

© 2002 Published by Elsevier Science Ltd.

Keywords: Stress; Three-dimensional; Notch

1. Introduction

The particular problems to be considered in this paper belong to a class of three-dimensional problems, which are closely related to the plane problems in the theory of elasticity. This class of problems may be described as follows. Consider a homogeneous, isotropic, elastic body bounded by two parallel planes, as well as by one or several cylindrical surfaces whose generators are perpendicular to the bounding planes. Let the body be subjected to surface tractions on the cylindrical boundaries or infinity, and, furthermore, let these tractions be parallel to the bounding planes and constant along any particular generator of the lateral boundary. According to the Michell theory (1899), in the limiting cases of very thin plate and very thick plate, corresponding respectively to plane-stress and plane-strain conditions, the three-dimensional

* Corresponding author. Tel.: +61-3-9626-7125; fax: +61-3-9626-7089.

E-mail address: chun.wang@dsto.defence.gov.au (C.H. Wang).

governing equations of the problem produce identical solutions for the in-plane stresses. For intermediate plate thickness, the exact solution is known to consist of an interior component and layer components (Gregory and Wan, 1988). While the interior solution is significant throughout the plate, the layer solution has only a localised effect in regions near plate edges. Nevertheless, it has been confirmed by several numerical computations that the corresponding plane solutions of the theory of elasticity provide a good approximation to the in-plane stresses. However, it is also well recognised that these plane solutions are not applicable when assessing the out-of-plane stress and deformation (Sternberg and Sadowsky, 1949; Young and Sternberg, 1966; Folias and Wang, 1990; Krishnaswamy et al., 1998; Li et al., 2000, 2001).

The actual three-dimensional stress and deformation fields near a curved boundary are very complex and there are only few analytical three-dimensional solutions available in the literature for non-trivial geometries and particular boundary conditions. These particular solutions give a little help in the analysis of practical problems of finite thickness plates with cut-outs of irregular shape. To develop rigorous analytical solutions a number of approximate theories (Sternberg and Sadowsky, 1949; Gregory and Wan, 1988) have been developed to take into account the effects of three-dimensional constraint around a stress concentrator. Many of these theories are based on an asymptotic expansion with respect to a small parameter, which is usually the ratio of the thickness to a characteristic length of the problem. However, it is clear that the underlying assumption confines the validity of any solutions obtained within these theories to only small values of the chosen parameter, i.e., for relatively thin plates. Since these theories are treated exhaustively in the literature we merely cite the main results, which are important for our purposes.

Analytical as well as numerical investigations reported in the literature showed that there is only a slight difference between the in-plane stresses obtained from plane-strain theory and three-dimensional finite element methods. For example, the increase in the stress concentration factor K_t for an infinite plate with a through-the-thickness hole subjected to uniaxial loading is less than 3% (Sternberg and Sadowsky, 1949). Nevertheless the out-of-plane constraint defined as the ratio of out-of-plane stress to the sum of in-plane stresses at the mid-plane,

$$C_z = \frac{\sigma_{zz}}{v(\sigma_{xx} + \sigma_{yy})} \quad (1)$$

is strongly dependent on the plate thickness (relative to the hole radius) and can vary between 0 (plane-stress) and 1 (plane-strain). In the case of elastic deformation, this out-of-plane constraint has only minor effect on the in-plane stress distribution. However, when plastic yielding occurs at a notch root, this three-dimensional constraint has a significant influence on the notch-tip stress state. For instance, the in-plane stress directly ahead of a notch root can exceed the material's yield stress by up to 70% under plane-strain conditions (Wang et al., 1999). Approximate methods (Ball, 1999) have been proposed to account for the effect of three-dimensional constraint on the elastic–plastic deformation at notch root by introducing this constraint factor C_z into existing two-dimensional analysis. However, such an approach would require a prior knowledge of this constraint factor for a given notch configuration, which is yet unavailable in the literature.

For the case of wave motion in plates, an approach, which does not introduce a small parameter as in perturbation solutions and includes the possibility of large transverse shear stress, while still retaining the simplicity of a two-dimensional model, was introduced by Kane and Mindlin (1956). In this paper this theory will be denoted as the generalised plane-strain theory. This method has also been exploited by Yang and Freund work (1985) to study the effect of transverse shear effects for through-cracks in an elastic plate. Using the same formulation, Krishnaswamy et al. (1998) investigated the stress concentration in elastic Cosserat plates with a circular hole undergoing extensional deformations. However, their results of the stress concentration factor of a circular hole under uniaxial tension approached two in the thick plate limit. These incorrect results led Krishnaswamy et al. to conclude that the Kane–Mindlin theory may be invalid for thick plates.

The purpose of the present work is to present an exact solution, obtained using the Kane and Mindlin's generalised plane-strain theory, of the stress concentration factor for finite thickness plate containing a circular hole subjected to remote tension and shear loading. It will be shown that, contrary to the work of Krishnaswamy et al. (1998), the present solution of the stress concentration factor for a circular hole in an infinite plate recovers correctly the plane-stress and plane-strain solutions in the thin and thick plate limits. For intermediate ratio of plate thickness to hole radius, the present result of the in-plane stress concentration factor is only slightly perturbed from the plane-strain result. The out-of-plane constraint, defined by Eq. (1), on the other hand, increases rapidly as the ratio of the plate thickness to the hole radius increases, approaching the plane-strain limit of unity. An approximate solution is also presented for a deep notch with a circular tip by making use of the known plane-strain solution of the problem, which is shown to compare well with published finite element solutions.

2. Governing equations of the generalised plane-strain theory

The theory of generalised plane-strain (Kane and Mindlin, 1956) assumes that the through-the-thickness extensional strain is uniform in the thickness direction. In the case of an elastic plate bounded by planes $z = \pm h$, where x and y represent the in-plane Cartesian coordinates (Fig. 1), the displacement field takes the following form:

$$u_x = u_x(x, y), \quad u_y = u_y(x, y), \quad u_z = \frac{z}{h} w(x, y). \quad (2)$$

It is clear that Eq. (2) implies that lines normal to the mid-plane of the plate in the undeformed state remain normal to the mid-plane in the deformed state and that these lines experience uniform extensional strain $w(x, y)/h$, where $w(x, y)$ is the out-of-plane displacement of the surface $z = h$ of the plate. It is noted that with the displacement field given by Eq. (2), all the stress components are linearly distributed in the thickness (z) direction.

With the generalised plane-strain theory, the three-dimensional field equations reduce to a set of two-dimensional governing equations. This procedure has been illustrated by Kane and Mindlin (1956) in their work on high-frequency extensional vibration of plates where material inertia has been taken into account. The system of field equations in the absence of the body forces and inertia effects can be obtained from Kane and Mindlin's work by setting the mass density to zero. To facilitate the following analysis, the stress resultants are defined by

$$(N_{xx}, N_{yy}, N_{zz}, N_{xy}) = \int_{-h}^h (\sigma_{xx}, \sigma_{yy}, \sigma_{zz}, \tau_{xy}) dz, \quad (3)$$

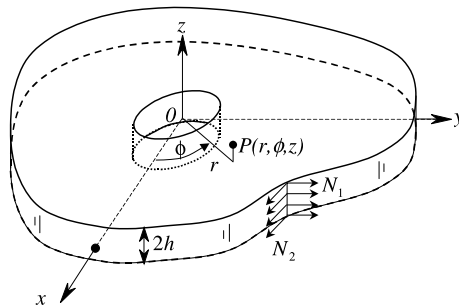


Fig. 1. Geometry of a plate with a notch, showing Cartesian and cylindrical co-ordinate systems.

$$(R_x, R_y) = \int_{-h}^h (\tau_{zx}, \tau_{zy}) z \, dz. \quad (4)$$

It is seen that the N_{xx} , N_{yy} , and N_{xy} are the usual forces per unit length, and N_{zz} is $2h$ times the average transverse normal stress. Parameters R_x and R_y are components of “pinching” shear moment, playing a role similar to that of the transverse shear force in the corresponding equilibrium equations of flexible plates. The equilibrium equations, in the absence of body forces and inertia effects, can now be expressed in terms of stress resultants and “pinching” shears, by substituting Eqs. (3) and (4) into the three-dimensional field equations and then integrating with respect to z between the limits $\pm h$ (Kane and Mindlin, 1956), except that the equilibrium equation for z -direction is first multiplied by z before integrating through the plate thickness,

$$\frac{\partial N_{xx}}{\partial x} + \frac{\partial N_{xy}}{\partial y} = 0, \quad \frac{\partial N_{xy}}{\partial x} + \frac{\partial N_{yy}}{\partial y} = 0, \quad \frac{\partial R_x}{\partial x} + \frac{\partial R_y}{\partial y} - N_{zz} = 0. \quad (5)$$

Making use of Hooke's law, the stress resultants and the shear components can be expressed in terms of the displacement components, setting the shear correction factor to be unity,

$$N_{\alpha\beta} = 2h[\lambda\theta\delta_{\alpha\beta} + \mu(u_{\alpha,\beta} + u_{\beta,\alpha})], \quad (6a)$$

$$N_{zz} = 2h\left[\lambda\theta + 2\mu\frac{w}{h}\right], \quad (6b)$$

$$R_x = \frac{2h^2}{3}\mu\frac{\partial w}{\partial x}, \quad R_y = \frac{2h^2}{3}\mu\frac{\partial w}{\partial y}, \quad (6c)$$

where the Greek indices $(\alpha, \beta) = (x, y)$, and the summation rule applies for repeated indices. The parameter θ denotes the volume strain,

$$\theta = \frac{\partial u_x}{\partial x} + \frac{\partial u_y}{\partial y} + \frac{w}{h}, \quad (7)$$

with λ and μ being the elastic constants, which are related to the Young's modulus E and Poisson's ratio ν via the following expressions:

$$\lambda = \frac{\nu E}{(1 + \nu)(1 - 2\nu)}, \quad \mu = \frac{E}{2(1 + \nu)}. \quad (8)$$

Denoting the mean in-plane stress resultant by

$$N = (N_{xx} + N_{yy})/2, \quad (9a)$$

the normal stress resultant N_{zz} can be expressed in terms of w and N as

$$N_{zz} = 2\nu N + 2Ew. \quad (9b)$$

It is clear that setting the shear correction factor to be unity is justified by the fact that the present result recovers the special case of plane-stress, i.e., $N_{zz} = 0$, because the out-of-plane displacement at the plate surface is

$$w = \varepsilon_{zz}h = -\frac{\nu}{E} \left(\frac{N_{xx}}{2} + \frac{N_{yy}}{2} \right) = -\frac{\nu}{E}N. \quad (10)$$

The first two equilibrium equations in (5) can be automatically satisfied by introducing a function Φ , similar to the Airy stress-resultant function,

$$N_{xx} = \frac{\partial^2 \Phi}{\partial y^2}, \quad N_{yy} = \frac{\partial^2 \Phi}{\partial x^2}, \quad N_{xy} = -\frac{\partial^2 \Phi}{\partial x \partial y}. \quad (11)$$

The third equilibrium equation in (5) yields, noting Eqs. (6c), (9a) and (9b),

$$\nabla^2 w - \frac{6(1+\nu)}{h^2} w = \frac{6\nu(1+\nu)}{h^2 E} N. \quad (12a)$$

The system of governing equations is completed by enforcing strain compatibility for the in-plane strain components (see Appendix A),

$$\nabla^2 N = \frac{\nu E}{1-\nu^2} \nabla^2 w, \quad (12b)$$

where condition (9b) has been used.

It is clear that by contrast to the two-dimensional plane-stress theory, the mean stress resultant N according to the present theory is not a harmonic function, i.e., $\nabla^2 N \neq 0$. Combining Eqs. (12a) and (12b) yields the following governing equation for the out-of-plane displacement w ,

$$\nabla^4 w - \kappa^2 \nabla^2 w = 0, \quad (13)$$

with

$$\kappa = \frac{1}{h} \sqrt{\frac{6}{1-\nu}}. \quad (14)$$

It is readily shown that the stress-resultant function is related to the out-of-plane displacement via the following equation, because $\nabla^2 \Phi = 2N$ according to Eqs. (9a) and (11),

$$\nabla^4 \Phi = \frac{2\nu E}{1-\nu^2} \nabla^2 w. \quad (15)$$

It is also clear that the stress-resultant function Φ is not bi-harmonical, i.e., $\nabla^4 \Phi \neq 0$, except in the special cases of plane-stress ($\nabla^2 N = 0$ hence $\nabla^2 w = 0$) or plane-strain deformation ($w = 0$). This also clearly shows that the present theory correctly recovers, as special cases, the solutions of plane-strain and plane-stress.

Eqs. (13) and (15) furnish a set of coupled equations for the out-of-plane displacement w and the stress-resultant function Φ , while the normal stress resultant N_{zz} can be found from (9a) and (9b). The boundary conditions are normally given in terms of the in-plane stress resultants $N_{\alpha\beta}$, which are determined separately by the stress-resultant function (11),

$$N_{\eta\eta} = \bar{N}_{\eta\eta}, \quad N_{\xi\eta} = \bar{N}_{\xi\eta}, \quad R_\eta = 0, \quad (16)$$

where the barred quantities are known quantities and co-ordinate system is a right-hand system with ξ measuring along the boundary and η in the direction of outward normal. The last boundary condition for the function w just means the absence of the transverse shear stress on the boundaries of the body under consideration (see Eq. (6c)).

3. General solutions for an annulus

The particular problem to be treated subsequently consists of determining the stress resultants throughout an annulus, with inner and outer radii being respectively a and b , and thickness being $2h$. The annulus is subjected to arbitrary tractions along its inner and outer edges that can be represented by the Fourier series. In the following only the solution for the cosine series will be presented; the results for the sine series can be derived in a similar manner. For symmetric loading against the y -axis, it suffices to

consider only cosine series of the stress-resultant function. The corresponding boundary conditions can be expressed as

$$N_{rr}(a) = \sum_{n=0}^{\infty} \bar{N}_{rr}^{an} \cos(n\phi), \quad N_{rr}(b) = \sum_{n=0}^{\infty} \bar{N}_{rr}^{bn} \cos(n\phi), \quad (17a)$$

$$N_{r\phi}(a) = \sum_{n=0}^{\infty} \bar{N}_{r\phi}^{an} \sin(n\phi), \quad N_{r\phi}(b) = \sum_{n=0}^{\infty} \bar{N}_{r\phi}^{bn} \sin(n\phi), \quad (17b)$$

$$R_r(a) = 0, \quad R_r(b) = 0, \quad (17c)$$

where bared quantities are constants.

Without losing generality, solution of the out-of-plane displacement $w(r, \phi)$ can be expressed as

$$w = \sum_{n=0}^{\infty} w_n(r) \cos(n\phi), \quad (18a)$$

which implies that the mean in-plane stress resultant and the stress-resultant function can be expressed as

$$N = \sum_{n=0}^{\infty} N_n(r) \cos(n\phi), \quad (18b)$$

$$\Phi = \sum_{n=0}^{\infty} \Phi_n(r) \cos(n\phi). \quad (18c)$$

Recalling the strain compatibility Eq. (12b), the mean stress resultant can be expressed in terms of the out-of-plane displacement,

$$N_n(r) = \frac{vE}{1-v^2} (w_n + A_{n1}r^{-n} + A_{n2}r^n), \quad (19)$$

where A_{n1} and A_{n2} are constants to be determined later. Substituting (19) into (12a) leads to, after simplifying the coefficients,

$$\frac{d^2 w_n}{dr^2} + \frac{1}{r} \frac{dw_n}{dr} - \left(\kappa^2 + \frac{n^2}{r^2} \right) w_n = \kappa^2 v^2 (A_{n1}r^{-n} + A_{n2}r^n). \quad (20)$$

Applying the method of variation of parameters to the above equation, the function w can be written in the form:

$$w_n(r) = -v^2 (A_{n1}r^{-n} + A_{n2}r^n) + A_{n3}K_n(\kappa r) + A_{n4}I_n(\kappa r), \quad (21)$$

where A_{n3} and A_{n4} are constants yet to be determined, K_n and I_n are the modified Bessel functions of n th order.

In the cylindrical co-ordinate system the stress resultants are given by

$$N_{rr} = \frac{1}{r} \frac{\partial \Phi}{\partial r} + \frac{1}{r^2} \frac{\partial^2 \Phi}{\partial \phi^2}, \quad (22a)$$

$$N_{\phi\phi} = \frac{\partial^2 \Phi}{\partial r^2}, \quad (22b)$$

$$N_{r\phi} = -\frac{\partial}{\partial r} \left(\frac{1}{r} \frac{\partial \Phi}{\partial \phi} \right). \quad (22c)$$

Recalling Eq. (15), the governing equation for Φ_n becomes

$$\frac{d^2\Phi_n}{dr^2} + \frac{1}{r} \frac{d\Phi_n}{dr} - \frac{n^2}{r^2} \Phi_n = 2N_n(r), \quad (23)$$

with $N_n(r)$ being given by the following expression, noting Eqs. (19) and (21),

$$N_n(r) = \frac{vE}{1-v^2} [(1-v^2)(A_{n1}r^{-n} + A_{n2}r^n) + A_{n3}K_n(kr) + A_{n4}I_n(kr)]. \quad (24)$$

The solution of Eq. (23) can be obtained by the method of variation of parameters,

$$\Phi_n(r) = -\frac{1}{n} \left[r^n \int_r^b \xi^{1-n} N_n(\xi) d\xi + r^{-n} \int_a^r \xi^{1+n} N_n(\xi) d\xi \right] + A_{n5}r^{-n} + A_{n6}r^n, \quad (25)$$

for $n = 1, 2, 3, \dots$. Here a and b are inner and outer radii of the circular region and ξ is merely the dummy variable of integration. For each angular parameter n , there are six boundary conditions given by Eqs. (17a)–(17c), so that the all the integration constants can be fully determined.

4. An infinite plate with a circular hole undergoing extensional deformations

As an example of the application of the solution obtained in the previous section, consider an infinite plate of thickness $2h$ with a circular hole of radius a , which is subjected to a uniform state of stress parallel to the mid-plane of the plate. In this case the constants A_{22} , A_{24} , and A_{26} in relationships (21) and (25) are equals to zero. The remaining three constants A_{21} , A_{23} , and A_{25} can be determined from the boundary conditions.

Solution of this problem may be reached by superposition of the solution corresponding to the following two basic loading cases: plane hydrostatic state of stress and plane state of pure shearing stress. In the first case the solution in cylindrical co-ordinates is given by

$$N_{rr} = \bar{N}_1 \left(1 - \frac{1}{r^2} \right), \quad N_{\phi\phi} = \bar{N}_1 \left(1 + \frac{1}{r^2} \right), \quad R_\phi = 0, \quad (26)$$

where \bar{N}_1 is a constant. We note that the Eq. (26) also represents the exact three-dimensional solution. Thus, we only need to obtain a solution for the second (pure shear) case of loading, described by the following boundary conditions at infinity:

$$N_{rr} = -\bar{N}_2 \cos(2\phi), \quad N_{\phi\phi} = \bar{N}_2 \cos(2\phi), \quad N_{r\phi} = \bar{N}_2 \sin(2\phi). \quad (27)$$

In this case we represent the solution as a sum of the pure shear state of an infinite plate without the hole and the solution for an infinite plate with the hole when the boundary conditions are prescribed on the edge of the hole,

$$N_{rr}(a) = \bar{N}_2 \cos(2\phi), \quad N_{r\phi}(a) = -\bar{N}_2 \sin(2\phi), \quad R_\phi(a) = 0, \quad (28)$$

where \bar{N}_2 is a constant that is not important in our further consideration because all results will be presented in the non-dimensional form. Solutions for the out-of-plane displacement, the mean stress resultant, and the stress-resultant function are, because all other terms ($n \geq 3$) are zero,

$$w = [-A_{21}v^2r^{-2} + A_{23}K_2(kr)] \cos(2\phi), \quad (29a)$$

$$N = \frac{vE}{1-v^2} [A_{21}(1-v^2)r^{-2} + A_{23}K_2(kr)] \cos(2\phi), \quad (29b)$$

$$\Phi(r) = \left[\frac{A_{25}}{r^2} - \frac{r^2}{2} \int_r^\infty \xi^{-1} N(\xi) d\xi - \frac{1}{2r^2} \int_a^r \xi^3 N(\xi) d\xi \right] \cos(2\phi). \quad (29c)$$

The three integration constants A_{21} , A_{23} , and A_{25} are now to be determined from the boundary conditions (28), yielding the following solutions:

$$A_{21} = \frac{2(1-v^2)\kappa^2 a^4 [K_1(\kappa a) + K_3(\kappa a)]}{vE\{8v^2K_1(\kappa a) + (1-v^2)\kappa^2 a^2 [K_1(\kappa a) + K_3(\kappa a)]\}} \bar{N}_2, \quad (30a)$$

$$A_{23} = \frac{8v(1-v^2)\kappa a}{E\{8v^2K_1(\kappa a) + (1-v^2)\kappa^2 a^2 [K_1(\kappa a) + K_3(\kappa a)]\}} \bar{N}_2, \quad (30b)$$

$$A_{25} = 0. \quad (30c)$$

Superimposition of the solutions (27) and (29a)–(29c) leads to the final stress resultants for an infinite plate with circular hole subjected to a remote shear loading. In particular, the maximum hoop stress at the hole edge, $N_{\phi\phi,\max}$, is given by

$$N_{\phi\phi,\max} = 2N(r=a, \theta=0), \quad (31)$$

from which the stress concentration factor can be readily derived,

$$K_{T,\text{shear}} = \frac{N_{\phi\phi,\max}}{\bar{N}_2} = \frac{4\kappa a[\kappa a(1-v^2)K_1(\kappa a) + 2K_2(\kappa a)]}{[4v^2 + \kappa^2 a^2(1-v^2)]K_1(\kappa a) + 2\kappa a(1-v^2)K_2(\kappa a)}. \quad (32)$$

Fig. 2a shows the variation of this stress concentration factor for different plate thickness. It can be seen that the stress concentration factor $K_{T,\text{shear}}$ increases with Poisson's ratio but the maximum stress concentration factor does not exceed ten percent of the corresponding plane-stress solution, where it is equal to 4.

For the technically more significant loading of uniaxial tension at infinity ($N_{xx}=0$, $N_{yy}=N^\infty$), the solutions can be readily obtained by superposition, Eq. (26) with $\bar{N}_1=(1/2)N^\infty$, and Eq. (28) with $\bar{N}_2=(1/2)N^\infty$. The maximum stress concentration factor $K_{T,\text{tension}}$ at the hole edge ($\phi=0$) can then be expressed as

$$K_{T,\text{tension}} = 1 + \frac{K_{T,\text{shear}}}{2}, \quad (33)$$

which is shown in Fig. 2(b). It can be seen for a Poisson's ratio of 0.3, the maximum stress concentration factor is only about 2% above the plane-stress solution, and therefore the influence of plate thickness can be ignored for engineering applications.

Within the generalised plane-strain theory, the out-of-plane stress constraint defined by Eq. (1) can be expressed in terms of the mean stress resultants,

$$C_{z,\text{shear}} = \frac{N_{zz}}{v(N_{xx} + N_{yy})} = \frac{N_{zz}}{2vN} = 1 + \frac{E}{v} \frac{w}{N}. \quad (34)$$

With the constants given by Eqs. (29a)–(29c) and (30a)–(30c), an explicit solution of the out-of-plane stress constraint factor can be obtained as follows:

$$C_{z,\text{shear}} = \frac{4r^2 K_2(kr)}{\kappa a^3(1-v^2)[K_1(\kappa a) + K_3(\kappa a)] + 4v^2 r^2 K_2(kr)}, \quad r \geq a. \quad (35)$$

It is readily seen that the constraint factor is dependent on the Poisson's ratio and the ratio a/h only. It is worth noting that the out-of-plane constraint factor is constant around the hole boundary, i.e., independent

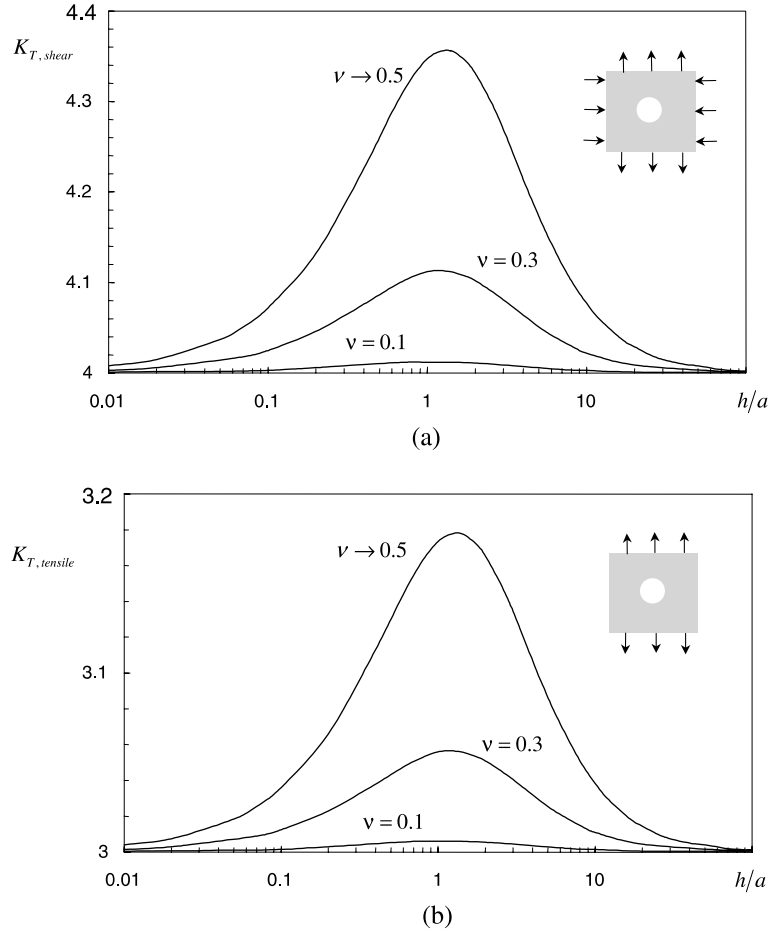


Fig. 2. The stress concentration as a function of ratio of the half-thickness to radius for an infinite plate with a circular hole subjected to (a) shear loading and (b) uniaxial tension.

of the angle ϕ . Fig. 3(a) shows the dependence of this constraint factor on the ratio of half-thickness to hole radius.

For the case of uniaxial tension at infinity ($N_{xx} = 0, N_{yy} = N^\infty$), since the plate thickness has a very minor influence on the in-plane stress concentration, as shown in Fig. 2(b), a good approximate solution of the out-of-plane constraint factor can be obtained similar to (32) from the superposition principle as follows:

$$C_{z,\text{tension}} = \frac{2}{K_{T,\text{tension}}} C_{z,\text{shear}} \approx \frac{2}{3} C_{z,\text{shear}}. \quad (36)$$

Since the maximum value of $C_{z,\text{shear}}$ is unity in the plane-strain limit, the present solution suggests that the maximum out-of-plane constraint does not exceed $2/3$, which is consistent with the exact plane-strain value of $\lim_{h/a \rightarrow \infty} \sigma_z = 2\nu$ (Sternberg and Sadowsky, 1949).

As seen in Fig. 4 that Poisson's ratio has a little effect on the maximum constraint factor, which depends strongly on the ratio of half-plate thickness to the hole radius. To further illustrate this point, distributions of the out-of-plane constraint factor for three different Poisson's ratios are plotted in Fig. 4, where the

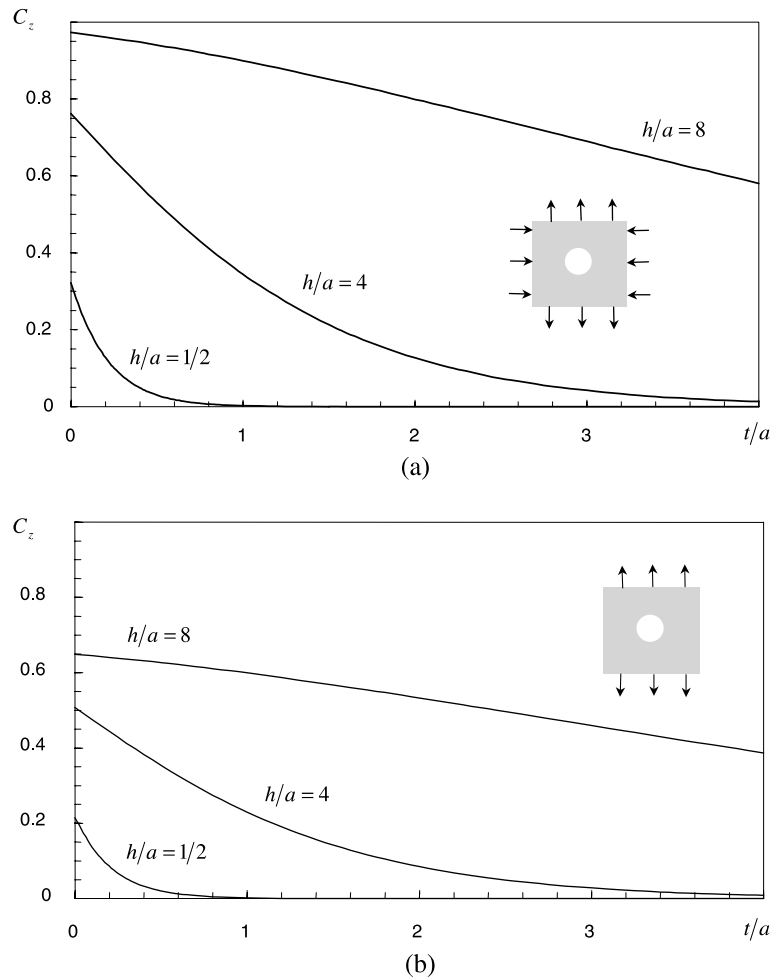


Fig. 3. The out-of-plane constraint factor of plate with a circular hole subjected to (a) shear loading and (b) uniaxial tension. Poisson's ratio is 0.3. The parameter t denotes the distance from the edge of the hole.

$h/a = 2$. These results clearly show that the Poisson's ratio has only a minor influence on both the maximum value and the distribution of the stress constraint factor.

5. V-shaped notch with a circular tip

As it has been shown earlier for the case of circular hole the transverse shear effect has a small influence on the in-plane stress field. This is also true for other notch configurations (Li et al., 2000, 2001). Therefore it is possible to obtain with a high level of accuracy the out-of-plane displacement ω , and hence the out-of-plane constraint, by approximating the mean in-plane stress resultant N using two-dimensional plane-stress solution, i.e.,

$$N \approx 2h\sigma_m, \quad (37)$$

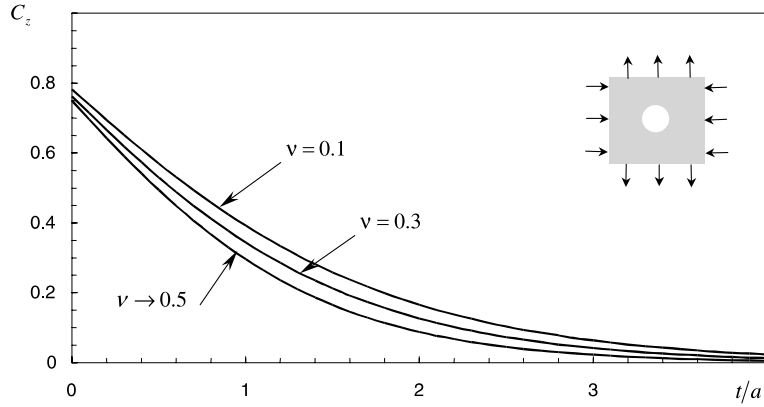


Fig. 4. Out-of-plane constraint factor as a function of the distance (t) from the edge of the hole (radius = a) showing the effect of Poisson's ratio in the case of the pure shear loading ($h/a = 2$).

where $\sigma_m = (\sigma_{xx} + \sigma_{yy})/2$ is the plane solution of the problem. Consider a semi-infinite plate with a deep notch, which has a circular tip of radius ρ , subjected to remote tension at the infinity, as shown in Fig. 5. The two-dimensional solution of this problem results in a unique stress distribution near the notch root (Lazzarin and Tovo, 1996), with the magnitude being proportional to the applied load. The mean stress for mode I (tension) can be written in the form:

$$\sigma_m = B_1 r^{\lambda_1 - 1} \cos[(1 - \lambda_1)\phi]. \quad (38)$$

Similarly, the mean stress under remote shear mode loading can be expressed as

$$\sigma_m = B_2 r^{\lambda_2 - 1} \sin[(1 - \lambda_2)\phi], \quad (39)$$

where parameters B_1 and B_2 are dependent on the applied load and notch geometry, λ_1 and λ_2 are the eigenvalues with the smallest real parts of the following characteristic equations:

$$\sin[\lambda_1(2\pi - 2\gamma)] + \lambda_1 \sin(2\pi - 2\gamma) = 0 \quad (\text{tensile mode}), \quad (40)$$

and

$$\sin[\lambda_2(2\pi - 2\gamma)] - \lambda_2 \sin(2\pi - 2\gamma) = 0 \quad (\text{shear mode}), \quad (41)$$

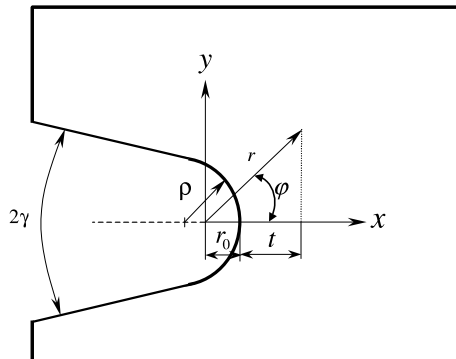


Fig. 5. Co-ordinate systems and notations for a V-shaped notch with a circular tip.

and the origin of the co-ordinate system is centred at a distance r_0 behind the notch tip,

$$r_0 = \frac{\pi - 2\gamma}{2\pi - 2\gamma} \rho. \quad (42)$$

It is worth noting that, according to the present theory, the order of singularity for a sharp V-notch in a plate of arbitrary thickness remains the same as that corresponding to plane-stress or plane-strain, which are the same (Williams, 1952). Plots of λ_1 and λ_2 as a function of the notch opening angle 2γ are available, for example in (Williams, 1952; Lazzarin and Tovo, 1996). Consequently from (21), the approximate solution of the problem will involve the modified Bessel functions of $1 - \lambda_1$ or $1 - \lambda_2$ order.

A first order solution for the out-of-plane constraint factor can be obtained by approximating $N(r, \phi)$ to have the same angular dependence as the corresponding plane-stress solution,

$$N(r, \phi) = N_n(r) \cos(n\phi), \quad n = 1 - \lambda_1, \quad \text{for mode I,} \quad (43)$$

and

$$N(r, \phi) = N_n(r) \sin(n\phi), \quad n = 1 - \lambda_2, \quad \text{for mode II.} \quad (44)$$

It should be pointed out no assumption has been made about the function $N_n(r)$, which should be determined from the governing equations using the method outlined in the previous section. In particular, the mean in-plane stress resultant N and the out-of-plane displacement ω are given by Eqs. (21) and (24), with the two integration constants $A_{n2} = 0$ and $A_{n4} = 0$. In particular, the mean in-plane stress resultant and the out-of-plane displacement are,

$$N_n(r) = \frac{vE}{1 - v^2} [A_{n1}(1 - v^2)r^{-n} + A_{n3}K_n(\kappa r)] \cos(n\phi), \quad (45a)$$

$$\omega_n(r) = [-A_{n1}v^2r^{-n} + A_{n3}K_n(\kappa r)] \cos(n\phi). \quad (45b)$$

The two constants A_{n1} and A_{n3} can be determined from the following boundary conditions:

$$N_n(r = r_0) = \bar{N}_t, \quad (46a)$$

$$\left. \frac{dw_n(r)}{dr} \right|_{r=r_0} = 0, \quad (46b)$$

where \bar{N}_t denotes the mean in-plane stress resultant at the tip of the notch. The solutions of the constants are,

$$A_{n1} = \bar{N}_t \frac{(1 - v^2)\kappa r_0^{1+n}[K_{n-1}(\kappa r_0) + K_{n+1}(\kappa r_0)]}{vEH}, \quad (47a)$$

$$A_{n3} = \bar{N}_t \frac{2nv(1 - v^2)}{EH}, \quad (47b)$$

with

$$H = (1 - v^2)\kappa r_0[K_{n-1}(\kappa r_0) + K_{n+1}(\kappa r_0)] + 2nv^2K_n(\kappa r_0). \quad (47c)$$

The fact that the constant A_{n3} is not zero indicates that the mean in-plane stress resultant differs from the plane-stress solution, which is similar to the findings by Yang and Freund (1985) for the case of a tensile crack in a finite thickness plate. However, the difference, which is given by the modified Bessel function K_n diminishes rapidly as the distance increases from the notch root, so that the plane-stress is asymptotically approached as large distance from the notch root.

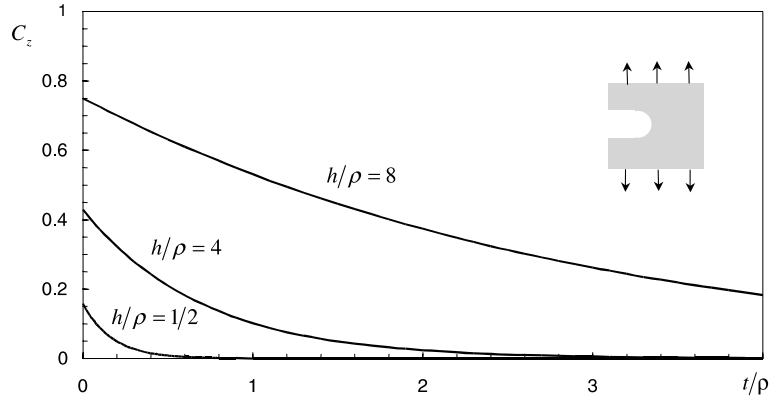


Fig. 6. The maximum constraint factor at notch root ($\phi = 0$) as a function of the distance t from the notch tip for various ratios of plate half-thickness h to notch root radius ρ ($\nu = 0.3$).

Now the out-of-plane stress constraint factor directly ahead of notch tip ($\theta = 0$) defined by (34) can be obtained as follows:

$$C_z(r) = \frac{2nr^n K_n(\kappa r)}{(1 - \nu^2)\kappa r_0^{1+n} [K_{n-1}(\kappa r_0) + K_{n+1}(\kappa r_0)] + 2n\nu^2 r^n K_n(\kappa r)}. \quad (48)$$

It is readily seen that this new solution recovers, as a special case ($n = 2$), the constraint factor for a circular hole given by Eq. (35).

Consider the case of a parallel slit with a round tip subjected to tensile loading. In this case the opening angle 2γ is zero, leading to $n = 1/2$ and $r_0 = (1/2)\rho$. The out-of-plane constraint factor now reduces to

$$C_z(t) = \frac{1}{(1 - \nu^2)(1 + \kappa\rho)e^{\kappa t} + \nu^2}, \quad (49)$$

where t ($= r - \rho/2$) denotes the distance ahead of the notch tip. The above solution is graphically shown in Fig. 6 for three different ratios of half-plate thickness to notch-tip radius. It is noted that both formulas for the constraint factor, Eqs. (35) and (49), exhibit proper behaviour in the limiting cases. For example, both the cases of plane-stress and plane-strain are recovered because $\lim_{h/a \rightarrow 0} C_z \rightarrow 0$ and $\lim_{h/\rho \rightarrow \infty} C_z \rightarrow 1$. It is also clear that plane-stress prevails at large distance from the notch root, i.e., $\lim_{r/\rho \rightarrow \infty} C_z \rightarrow 0$.

The out-of-plane constraint factor attains its peak value at the notch root ($t = 0$), where the constraint factor becomes,

$$C_z(t = 0) = \frac{1}{1 + (1 - \nu^2)\kappa\rho}. \quad (50)$$

It is clear that this constraint factor C_z depends only on Poisson's ratio and the ratio of notch-tip radius to the half-thickness of the plate (ρ/h). A comparison of the maximum constraint factors (directly ahead of notch tip $\phi = 0$) for the case of deep notch and the case of circular hole under uniaxial tension is presented in Fig. 7, together with the results of a finite element analysis (Li et al., 2000). Here the results of the finite element analysis are in terms of the constraint along the mid-plane of the plate. It is clear that although the present solution represents the average constraint through the plate thickness, the theoretical estimates compare very well with the computational results.

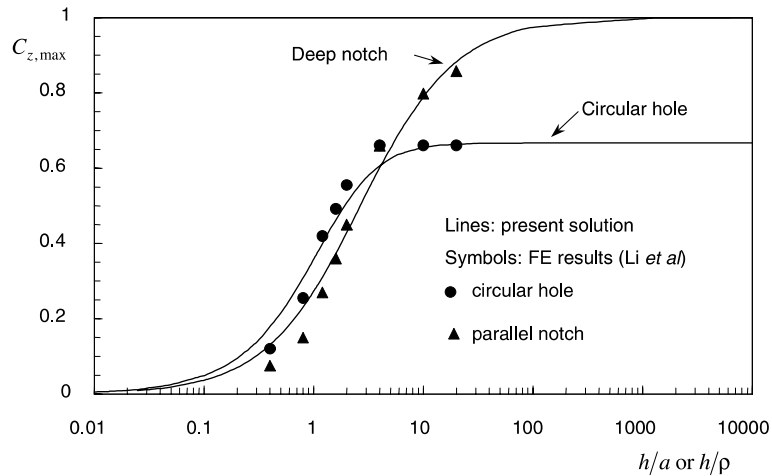


Fig. 7. The maximum constraint factor for the deep notch with zero opening angle and circular hole in an infinite plate under uniaxial tension versus the ratio of the plate's half-thickness to notch tip or hole radius (Poisson's ratio $\nu = 0.3$).

To further examine the distribution of the constraint factor ahead of the notch tip, a normalisation is introduced by dividing the constraint factor by its maximum value,

$$\frac{C_z(t)}{C_z(0)} = \frac{(1 - \nu^2)(1 + \kappa\rho) + \nu^2}{(1 - \nu^2)(1 + \kappa\rho)e^{\kappa t} + \nu^2} \approx e^{-\kappa t}. \quad (51)$$

It is clear that the normalised distribution, when plotted against the ratio of distance to the half-plate thickness, depends very weakly on Poisson's ratio and the ratio of notch root radius to plate thickness. This result is consistent with the finite element results of Li et al. (2000). A comparison between the present theoretical solution and the finite element results of Li et al. (2000) is shown in Fig. 8. It can be seen that the present theoretical solution correlates well with the numerical solution close to the notch root. However, the finite element results showed that the normalised constraint factor dips below zero at a distance of 0.375

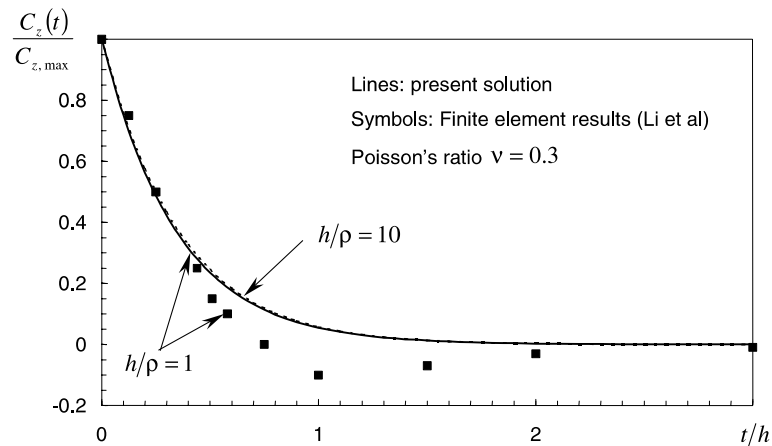


Fig. 8. Distribution of normalised constraint factor ahead of notch tip for uniaxial tension.

times the plate thickness ($t/h = 0.75$), while the present theory shows that the constraint factor remains positive. This may be due to that the finite element results are for the mid-plane values, rather the through-the-thickness average.

It is also worth noting that the present results confirm that the average of the through-the-thickness stress, i.e., N_{zz} is a monotone increasing function of the normalised plate thickness (h/ρ) which asymptotically approaches the plane-strain solution. Therefore the present method has overcome the convergence problem of the series expansion solution of Sternberg and Sadowsky (1949). The explicit solutions presented here are also very convenient for engineering applications as they can be readily implemented to provide an accurate estimate of the influence of plate thickness on the through-the-thickness stress constraint. The present solution method can be readily extended to sharp cracks, leading to possibly simpler solutions than those obtained by Yang and Freund (1985). This will be the subject of a separate article.

6. Conclusion

Based on the generalised plane-strain theory, which assumes that the through-the-thickness strain is uniform in the thickness direction, the three-dimensional governing equations have been reduced to a set of two-dimensional equations. These new governing equations permit an exact solution for an annulus with arbitrary edge loading, and for an infinite plate with a circular hole. The results show that, although the stress concentration factor for a circular hole in an infinite plate is only slightly perturbed from the plane-strain solution over a wide range of thickness to radius ratio, the out-of-plane constraint is strongly dependent on the ratio of plate thickness to radius.

By extending the method to non-circular holes, explicit formulae have also been derived for the out-of-plane constraint factor for V-shaped notches with circular tip. The present results have been validated by comparison against the results of finite element analyses, showing good correlation. It is shown that the out-of-plane constraint factor is strongly dependent on the ratio of plate thickness to notch-tip radius.

Acknowledgements

The authors would like to thank Drs. Dale Ball and Francis Rose for helpful discussions.

Appendix A

The strain compatibility equation for the in-plane strains is

$$\frac{\partial^2 \varepsilon_{xx}}{\partial y^2} + \frac{\partial^2 \varepsilon_{yy}}{\partial x^2} = \frac{\partial^2 \gamma_{xy}}{\partial x \partial y}. \quad (\text{A.1})$$

According to Hooke's law, using the present notation,

$$\varepsilon_{xx} = \frac{1}{2hE} (N_{xx} - vN_{yy} - vN_{zz}), \quad (\text{A.2})$$

$$\varepsilon_{yy} = \frac{1}{2hE} (N_{yy} - vN_{xx} - vN_{zz}), \quad (\text{A.3})$$

$$\gamma_{xy} = \frac{(1+v)}{hE} N_{xy}. \quad (\text{A.4})$$

Substituting Eqs. (A.2)–(A.4) into (A.1) yields,

$$\frac{\partial^2}{\partial y^2} (N_{xx} - vN_{yy}) + \frac{\partial^2}{\partial x^2} (N_{yy} - vN_{xx}) - v\nabla^2 N_{zz} = 2(1+v) \frac{\partial^2 N_{xy}}{\partial x \partial y}. \quad (\text{A.5})$$

From the equilibrium equations the following relationship can be derived:

$$2 \frac{\partial^2 N_{xy}}{\partial x \partial y} = - \frac{\partial^2 N_{xx}}{\partial x^2} - \frac{\partial^2 N_{yy}}{\partial y^2}. \quad (\text{A.6})$$

Therefore the compatibility Eq. (A.1) finally becomes,

$$\nabla^2 (2N - vN_{zz}) = 0. \quad (\text{A.7})$$

References

Ball, D., 1999. Fatigue crack growth analysis for localised plastic yielding problems, NASGRO Interagency Working Group (IWG) Meeting, NASA Johnson Space Centre, Houston, TX, 14–15 September, 1999.

Folias, E.S., Wang, J.J., 1990. On the three-dimensional stress field around a circular hole in a plate of arbitrary thickness. *Computat. Mech.* 6, 379–391.

Gregory, R.D., Wan, F.Y.M., 1988. The interior solution for linear problems of elastic plates. *J. Appl. Mech., Trans. ASME* 55, 551–559.

Kane, T.R., Mindlin, R.D., 1956. High frequency extensional vibrations of plates. *J. Appl. Mech., Trans. ASME* 23, 277–283.

Krishnaswamy, S., Jin, Z.H., Barta, R.C., 1998. Stress concentration in an elastic Cosserat plate undergoing extensional deformations. *J. Appl. Mech., Trans. ASME* 65, 66–70.

Lazzarin, P., Tovo, R., 1996. A unified approach to the evaluation of linear elastic fields in the neighborhood of cracks and notches. *Int. J. Fract.* 78, 3–19.

Li, Z., Guo, W., Kuang, Z., 2000. Three-dimensional elastic stress fields near notches in finite thick plates. *Int. J. Solids Struct.* 37, 7617–7631.

Li, Z., Guo, W., 2001. Three-dimensional elastic stress fields ahead of blunt V notches in finite thickness plate. *Int. J. Fract.* 107, 53–71.

Michell, J.H., 1899. On the direct determination of stress in an elastic solid, with application to the theory of plates. *Proc. Lond. Math. Soc.* 31, 100–124 (also in *The Collected Mathematical Works of J.H. and A.G.M. Michell*, edited by Niedenfuhr and Radok, Noordhoff Ltd, Groningen, the Netherlands, 1964).

Sternberg, E., Sadowsky, M.A., 1949. Three-dimensional solution for the stress concentration around a circular hole in a plate of arbitrary thickness. *J. Appl. Mech.* 16, 27–38.

Wang, C.H., Guo, W., Rose, L.R.F., 1999. A method for determining the elastic–plastic response ahead of a notch tip. *J. Eng. Mater. Technol.* 121, 313–320.

Williams, M.L., 1952. Stress singularities resulting from various boundary conditions in angular corners of strips in extension. *J. Appl. Mech.* 19, 526–528.

Yang, W., Freund, L.B., 1985. Transverse shear effects for through-crack in an elastic plate. *Int. J. Solids Struct.* 21, 977–994.

Young, C.K., Sternberg, E., 1966. Three-dimensional stress concentration around a cylindrical hole in a semi-infinite elastic body. *J. Appl. Mech.* 33, 855–865.